HHS Public Access

Author manuscript

Nat Struct Mol Biol. Author manuscript; available in PMC 2013 December 01.

Published in final edited form as:

Nat Struct Mol Biol. 2013 June ; 20(6): 740–747. doi:10.1038/nsmb.2568.

Studies of IscR reveal a unique mechanism for metal-dependent regulation of DNA binding specificity

Senapathy Rajagopalan[1], **Sarah J. Teter**[2], **Petrus H. Zwart**[3], **Richard G. Brennan**[4], **Kevin J. Phillips**[1,5,6], and **Patricia J. Kiley**[2]

[1]Genomic Medicine Program, The Methodist Hospital Research Institute, Houston, TX 77030

[2]Department of Biomolecular Chemistry, University of Wisconsin, Madison, WI, 53706

[3]Physical Biosciences Division, Lawrence Berkeley National Laboratory, Berkeley, CA 94720

[4]Department of Biochemistry, Duke University School of Medicine, Durham, NC 27710

[5]Diabetes Research Program, The Methodist Hospital Research Institute, Houston, TX 77030

[6]Department of Biology and Biochemistry, University of Houston, Houston, TX 77204

Abstract

IscR from *Escherichia coli* is an unusual metalloregulator in that it globally regulates transcription by recognizing two different DNA motifs in a Fe-S dependent manner. Here, we report structural and biochemical studies of IscR, which suggest remodeling of the protein-DNA interface upon Fe-S ligation broadens the DNA binding specificity from binding a type 2 motif to both type 1 and 2 motifs. Analysis of an apo-IscR variant with relaxed target-site discrimination identified a key residue in wild-type apo-IscR that we propose makes unfavorable interactions with a type 1 motif. Upon Fe-S binding, these interactions are apparently removed, thereby allowing holo-IscR to bind both type 1 and 2 motifs. These data suggest a novel mechanism of ligand-mediated DNA site recognition, whereby metallocluster ligation relocates a protein specificity determinant to expand DNA target site selection, allowing a broader transcriptomic response by holo-IscR.

INTRODUCTION

Fe-S proteins are ancient proteins found across all kingdoms of life. They play key structural, catalytic, or electron transfer roles in genome maintenance, transcription,

Correspondence to: Kevin J. Phillips, The Methodist Hospital Research Institute, Houston, TX, USA, Tel.:+1(713)441-2553; KPhillips@tmhs.org Correspondence to: Patricia Kiley, University of Wisconsin, Madison, WI, USA, Tel.:+1(608)262-6632; Fax:+1 (608)262-5253; pjkiley@wisc.edu.
S. Rajagopalan and S.J. Teter contributed equally to the work

Accession codes

4HF0 Structure of unbound apo-IscR
4HF1 Structure of IscR bound to the *hya* site
4HF2 Structure of IscR-E43A mutant bound to the *hya* site

Author Contributions

P.J.K., K.J.P., S.J.T., S.R. and R.G.B. designed the experiments. S.R., S.J.T. and P.H.Z. performed the experiments. P.J.K., K.J.P., S.J.T., and S.R. wrote the paper.

translation, and metabolism[1]. Recently, a number of regulatory proteins have been discovered that use Fe-S clusters as sensors of a variety of small molecules by exploiting the versatile chemical reactivity of these metal centers[2,3]. The regulatory response of the well-studied [4Fe-4S]-FNR regulator[2,3] is typical of most metalloregulators, in which binding of the cognate metal center converts the transcription factor between an inactive and active state and accordingly, changes expression of its regulon[4]. In contrast, the [2Fe-2S]-transcription factor IscR from *Escherichia coli*, has emerged as a novel type of regulator of gene expression, since both the clusterless (apo-IscR) and [2Fe-2S]-IscR are active transcriptional regulators[5–8]. Cluster ligation changes the DNA binding specificity to apparently alter the set of genes that IscR controls.

IscR is widely conserved in bacteria[9] and is part of the large Rrf2 family of transcription factors[9,10]. It was first discovered as the negative autoregulator of the *isc* operon that encodes IscR and members of the Isc Fe-S biogenesis pathway[11]. However, it is now known that IscR is a global regulator, directly or indirectly controlling expression of ~40 genes[12]. Analysis of IscR regulated genes revealed that IscR recognizes two different DNA binding motifs (referred to as type 1 and 2), depending on whether a [2Fe-2S] cluster is ligated to the protein[6,12]. Only [2Fe-2S]-IscR binds type 1 sites[5,8], whereas both [2Fe-2S]-IscR and apo-IscR bind a type 2 site with similar high affinity[6], indicating that the Fe-S cluster is not required for interaction with type 2 sites. The ability of IscR to discriminate between two DNA motifs was unexpected, since the predicted structure of IscR contains only a single winged helix-turn-helix DNA binding domain and because other known Fe-S cluster-containing transcription factors (e.g. FNR, SoxR) do not appear to regulate transcription when they lack a metal cluster[2,3,13–15]. The features of IscR target site recognition and the structural changes that alter the DNA binding specificity of IscR upon ligation of the [2Fe-2S] cluster are unknown.

To gain insight into how IscR recognizes two different DNA motifs, we used x-ray crystallography and structure-guided mutagenesis. We crystallized a mutant of IscR, which lacks the Fe-S cluster, bound to a well-studied type 2 site from the *hya* promoter. Based on the structure of the IscR-DNA protein complex, alanine substitutions were made to key residues mediating protein-DNA interactions, and the ability of these protein variants to recognize both type 1 and type 2 sites was determined using either [2Fe-2S]- or apo-IscR. We find that the side chain of Glu43 is a primary discriminator that allows apo-IscR to distinguish between a type 1 and type 2 binding site. These studies suggest a novel mechanism of metal-dependent regulation of a DNA binding transcription factor in which the DNA binding specificity is broadened by apparently repositioning a single key side chain upon ligation of the metal cofactor.

RESULTS

Structure of apo-IscR bound to a type 2 DNA site

We determined the crystal structure of IscR bound to a 29 base pair DNA fragment (*hya*) containing the type 2 binding site from the *hya* promoter using data extending to 2.22 Å resolution (Fig. 1A). To solve this structure, we used an IscR variant (IscR-3CA) in which the cluster coordinating cysteines (Cys92, Cys98, Cys104) were substituted to alanine,

ensuring that this protein lacked a Fe-S cluster[5,6]. IscR-3CA, hereafter referred to as IscR in the structural analysis, binds the *hya* site with similar affinity as wild-type IscR *in vitro* and is fully functional in repressing the *hya* promoter *in vivo*[6,8]. IscR was crystallized in the $P2_12_12_1$ space group, and the asymmetric unit contained an IscR homodimer bound to a single dsDNA from the *hya* site (Table 1). The two IscR subunits of the homodimer were nearly identical, with a root mean square deviation (rmsd) of 0.6Å.

IscR was primarily α-helical, comprised of two major structural elements: a DNA binding domain and a dimerization helix. Stabilization of the dimer was achieved principally through hydrophobic interactions between residues of the coiled-coil of the dimerization helix (residues103–123) as well as helices α1(residues 5–20) and α6(residues 126–134), burying ~3400 $Å^2$ of solvent accessible surface area between the two monomers. Helices α2(residues 25–32), α3(residues 36–42), β strands β1(residues 49–52), β2(residues 53–57), and the wing W1(residues 59–61) form the winged helix-turn-helix (wHTH) DNA recognition motif (Fig. 1B). The relatively long dimerization helix of IscR situated the DNA binding domains at the distal ends of the dimer, allowing the recognition helix, α3, of each monomer to interact with consecutive major grooves of the DNA and the wing to interact with adjacent minor grooves. This architecture was in agreement with the IscR DNA footprint of 27 base pairs[12] encompassing the two symmetry related half-sites shown by mutagenesis to be important for binding[6].

Electron density encompassing the residues that would be involved in [2Fe-2S] cluster ligation in wild-type IscR was apparent for only one of the two protein chains (Fig. 1A). The location of this electron density indicated that the cluster-binding site was solvent-exposed in this conformation. If this site was similarly positioned and solvent exposed in the ligand-bound form of IscR, then this location could allow for the facile incorporation and/or loss of the [2Fe-2S] cluster, providing a framework for understanding how this protein functions in sensing cellular Fe-S cluster status[8]. Additionally, the cluster-binding site from one subunit was proximal to the DNA binding domain of the other subunit, suggesting that Fe-S cluster ligation in one IscR subunit may influence the conformation and DNA binding of the other subunit.

The IscR-bound *hya* DNA was bent ~8.4° relative to ideal B-form DNA (Fig. 1C), while the overall DNA was slightly undertwisted (33.1° for *hya* compared to 35°–36° for the canonical B-DNA). Insertion of the recognition helix of IscR into the major groove widened the major groove from 11.0Å in B-form DNA to 14.3Å at nucleotide positions 9, 10, and 11. However, the overall DNA structure within the IscR-*hya* complex did not depart strikingly from ideal B-form DNA.

Recognition of the *hya* target site by apo-IscR

IscR possessed a basic surface, encompassing the recognition helix and the wing, which binds DNA (Supplementary Fig. 1). However, a salient feature of the IscR-DNA interface was the presence of a conserved glutamate, Glu43, in the middle of this basic DNA binding surface, which made a bidentate interaction between the carboxyl group of the side chain extending from the recognition helix and the exocyclic amines of C_7C_8 and $C_{7'}A_{8'}$ (Fig. 2 and Supplementary Fig. 1). Acidic residues are not typically involved in DNA base

recognition due to the potential for electrostatic repulsion with the electronegative DNA backbone; although, several examples, including CAP-DNA[16], RepE-DNA[17] and more commonly in zinc-cluster family protein-DNA complexes, have been reported[18]. In addition, the hydroxyl group of Ser40 of the recognition helix formed hydrogen bonds with N7 of A_{20} and $G_{20'}$, suggesting a rationale for the conservation of purines at position 20 in both half sites of the *hya* site. The side chain of Gln44, also of the recognition helix, formed a hydrogen bond with the carbonyl of T_{19} and $T_{19'}$ (Fig. 2), which is not as highly conserved in type 2 sites[6].

The structure also showed that the wing of the wHTH domain of IscR extended deeply into the minor groove of *hya* to provide additional specificity and stabilization (Fig. 2D). The Arg59-Gly60-Pro61 sequence of the wing interacted extensively with the A-T rich region of the *hya* site in a manner somewhat reminiscent of an A-T hook motif[19,20]. The side chain of Arg59 extended into the minor groove, while its guanidino group interacted with the carbonyl oxygens of T_6 and $T_{25'}$. The DNA bound structure of IscR provided insights into the GXXGG motif, which is conserved within both IscR orthologs and proteins in the larger Rrf2 family such as CymR[10]. Gly60 and Gly64 were found to be in conformations that lie in the glycine only region of Ramachandran space, disallowing their mutation to other residues, and consistent with the conservation of the $G_{60}XXG_{63}G_{64}$ motif within the wing. Additionally, the structure suggested that Gly60 and Gly63 must be glycine for steric reasons, as the presence of a Cβ carbon would create steric clashes between the wing and either the DNA or the β1 strand, respectively. Interestingly, while CymR shares the same structural features as IscR, such as unstructured regions between α4 and α5, identical residues in the recognition helix that make base-specific contacts in IscR, and similar overall folds, the length and spatial orientation of the dimerization helix is different (Supplementary Figure 2). Thus, while DNA recognition by CymR should be very similar to that of IscR, CymR binding likely requires a conformational change of either the protein, DNA or both, as Shepard et al[10] suggest.

Additional IscR-*hya* interactions included Tyr41, which formed a stacking interaction with the sugar moiety of G_{18} and a hydrogen bond with the backbone phosphate of the same nucleotide and may serve to expand the width of this region of the major groove to stabilize insertion of the recognition helix (Fig. 2). Tyr65 formed hydrogen bonds with the phosphates at position $C_{7'}$, while Arg2, Thr4, Ser5, Leu28, Ser38, Arg50, and Ser57 made additional contacts with the phosphate backbone (Fig. 2A).

Structural changes of IscR upon *hya* DNA binding

In order to assess the conformational changes that accompany the binding of IscR to the *hya* promoter, we also crystallized IscR in the absence of DNA (Fig. 3). The structure was obtained in the $P3_12_1$ space group and determined using data extending to 1.9 Å resolution (Table 1). Consistent with previous reports that IscR behaves as a dimer in solution[6], non-DNA-bound IscR crystallized as a homodimer. The similar oligomeric state of free and DNA-bound IscR indicated that regulation of IscR DNA binding is distinct from that of the FNR family of Fe-S transcription factors, for which cluster-induced dimerization commonly controls DNA binding[2,3,13].

Comparison of the structures of IscR in the unbound and DNA bound forms revealed that unbound IscR shared the same general structure as *hya*-bound IscR. The two subunits of the dimer were rotated by ~20° relative to each other, resulting in a 5.8 Å translation of the DNA recognition helix (α3) to position it in the major groove (Fig. 3). Aside from Glu43, which rotated upon binding to allow it to contact C_7C_8 and $C_{7'}A_{8'}$, only minor rotameric shifts were necessary to accommodate binding of IscR to the *hya* promoter. In general, residues of the IscR wing underwent little structural change upon DNA binding, except that the side chain of Arg59, for which no electron density was apparent in the unbound structure, became ordered upon binding to the minor groove of *hya*.

Residues involved in DNA interactions

The nucleotide bases that were contacted by the IscR side chains in the structure corresponded well to those that were previously identified as important for binding in mutational analysis of the *hya* site[6]. Furthermore, we rationalized the decrease in IscR binding affinity for the mutant *hya* sites as either removal of a nucleotide contact or a nucleotide sterically impeding the interaction of IscR side chains with DNA, which potentially obscures the contribution of some individual nucleotides in the *hya* site. To independently evaluate each side chain-nucleotide interaction, we removed side chain contacts by individually substituting Arg59, Tyr41, Ser40, Gln44, or Glu43 to alanine. We found that most variant IscR proteins bound the *hya* site with reduced affinity compared to the wild-type protein, demonstrating the crucial role of these side chains. We observed the largest defect upon alanine substitution of Arg59, indicating that the Arg59 side chain of the wing motif made a major contribution to binding affinity in part by forming an electrostatic interaction with the AT-rich minor groove (Table 2, Supplementary Fig. 3). A-T tracts of ≥ 3 base pairs are correlated with the presence of narrow minor grooves, which are often recognized by arginine residues[21,22]. This result was consistent with previous findings[6], which show that a GC base pair mutation within the AT-tract of the minor groove of the *hya* site abolishes IscR binding. Tyr41 also appeared to make a substantial contribution to DNA binding, since an alanine substitution at this position reduced binding affinity (Table 2,Supplementary Fig. 3). These results were consistent with Tyr41-DNA interactions providing binding energy to stabilize the recognition helix at the major groove.

We also found that removal of the side chains of three IscR residues that make base-specific interactions, Ser40, Gln44, and Glu43, had different effects on DNA binding affinity. Alanine substitution of Ser40 resulted in a moderate decrease in binding affinity (Table 2, Supplementary Fig. 3). Consistent with the role of the Ser40 side chain in recognition of the N7 of purines at 20 and 20', a purine to pyrimidine substitution at position 20 in the *hya* site abolishes IscR binding[6]. The Gln44 interaction with T_{19} and $T_{19'}$ did not appear to play a major role in recognition of the type 2 motif, since alanine substitution of Gln44 resulted in only a small defect in binding to the *hya* site (Table 2, Supplementary Fig. 3). Thymines at position 19 and 19' are poorly conserved in the type 2 motif (Supplementary Table 1), and mutations at these positions in the *hya* site also result in a mild binding defect[6]. Notably, alanine substitution of Glu43 had little effect on binding affinity (Table 2, Supplementary Fig. 3), despite the use of its carboxylate side chain to form hydrogen bonds with N4 of

C_7C_8 and N4 of $C_{7'}$ and N6 of $A_{8'}$ (Fig. 2B). This was a surprising result, since mutations at these positions in the *hya* site dramatically decrease binding of wild-type IscR[6].

IscR-E43A loses discrimination of the C_7C_8 dinucleotide

A possible explanation for the behavior of the E43A variant is that removal of the carboxylate side chain of Glu43 abolished specificity for these positions without altering binding affinity. Indeed, unlike wild-type IscR, IscR-E43A did not discriminate between nucleotide bases at positions 7 or 8, because mutations of C_7C_8 in one half site did not disrupt binding affinity as found with wild-type IscR (Table 3). These results suggested that Glu43 contacts are vital to recognition of the well-conserved CC dinucleotide in both half sites of type 2 sites. Additional competition binding experiments with IscR-E43A and mutant *hya* templates showed that despite losing specificity for the symmetrical CC dinucleotide, IscR-E43A retained the same specificity as wild-type IscR at other conserved positions in the *hya* site (data not shown) and bound to the *hya* site in the same manner as wild-type IscR, as shown by the structure of E43A-*hya* complex (Supplementary Fig. 4). Finally, one half site of *hya* contains $C_{7'}A_{8'}$, rather than the conserved CC dinucleotide. Mutation of $A_{8'}$ to cytosine slightly improved binding affinity (data not shown), consistent with the notion that the symmetrical CC dinucleotides recognized by Glu43 are preferred at positions 7 and 8 in both half sites of type 2 sites.

IscR uses Glu43 to discriminate against the type 1 motif

In contrast to IscR type 2 sites, type 1 binding sites are asymmetrical, containing the C_7C_8 dinucleotide in one half site and a $T_{7'}T_{8'}$ dinucleotide in the other half site (Table 3). Because apo-IscR binds to a type 2 motif but not a type 1 motif, we considered the possibility that an inhibitory interaction of Glu43 with the $T_{7'}T_{8'}$ dinucleotide in the type 1 motif prevented apo-IscR from binding. Therefore, we compared the ability of apo-IscR, [2Fe-2S]-IscR, as well as the apo and [2Fe-2S]-forms of IscR-E43A to bind to a type 1 site derived from the *isc* promoter, *iscRB*. As expected[6], apo-IscR bound the *iscRB* type 1 site poorly compared to [2Fe-2S]-IscR (Fig. 4). In contrast, apo-IscR-E43A strongly bound the *iscRB* type 1 site, comparable to [2Fe-2S]-IscR-E43A and wild-type [2Fe-2S]-IscR (Fig. 4). This affinity was also similar to that observed for apo- and [2Fe-2S]- IscR-E43A binding to the *hya* type 2 site, indicating that Glu43 does not contribute substantial binding energy to either type of site. Based on these observations, we propose that the apo-IscR residue Glu43 actively discriminates against asymmetrical dinucleotides at positions 7 and 8 that do not contain a major groove exposed exocylic amino group, as is the case in type 1 sites.

Differences in recognition of type 1 and type 2 motifs

Since eliminating the Glu43 side chain contacts allowed apo-IscR-E43A to bind the type 1 motif, we asked whether binding of wild-type apo-IscR to a type 1 site could be achieved by replacing the asymmetrical $T_{7'}T_{8'}$ dinucleotide with cytosines. To do this, we tested the ability of wild-type [2Fe-2S]- and apo-IscR to bind to an engineered symmetrical type 1 site (*iscRBcc*, Fig. 5A). Similar to IscR binding to the wild-type *iscRB* site, [2Fe-2S]-IscR bound *iscRBcc* with high affinity. However, apo-IscR bound poorly to the symmetrical *iscRBcc* site (Fig. 5B). Therefore, providing potentially favorable interactions with the CC dinucleotide

was not sufficient to allow high affinity apo-IscR binding with a type 1 site, suggesting that contacts to other nucleotides in the type 1 site are not made even when a CC dinucleotide is present in both half sites. This notion was supported by the fact that two additional nucleotides present in the *hya* type 2 site ($C_{10}A_{11}$ and $T_{10'}A_{11'}$), which were involved in specific interactions with the IscR side chains, are not conserved in the type 1 motif (Supplementary Table 1). Rather, the type 1 motif has A and C conserved at those positions, respectively.

If the observed differences in DNA sequence at the type 1 and type 2 motifs were functionally relevant, then the amino acid side chain requirements for binding the two motifs should also be different (Tables 2, 4, Supplementary Figs. 3, 5). Indeed, we found that the magnitude of the binding defects of only IscR-Q44A and IscR-S40A were different between the type 1 and type 2 sites. While the binding defect for the Q44A variant was greater for the type 1 site than the type 2 site, the S40A variant was opposite, showing a smaller binding defect for a type 1 site than a type 2 site. Thus these data suggested that the side chains of Gln44 and Ser40 are likely to be involved in different specificity-determining contacts at the two sites.

We also found that substitution of Tyr41 or Arg59 with alanine caused a substantial binding defect at both type 1 and type 2 sites, suggesting that IscR uses these side chains in binding of both sites (Tables 2, 4, Supplementary Figs. 3, 5). Consistent with this notion, an AT-rich region for binding the wing motif is also conserved in the type 1 site (Supplementary Table 1). In summary, while IscR uses one DNA binding interface to recognize similar structural features of both type 1 and 2 motifs, it is apparent that nucleotide base recognition, in particular the recognition of a CC dinucleotide at positions 7 and 8 in both half sites by the Glu43 side chain, allows apo-IscR to discriminate between type 1 and 2 sites.

DISCUSSION

While IscR was first discovered as the negative autoregulator of the *E. coli isc* operon, which encodes IscR and members of the Isc Fe-S biogenesis pathway[11], it is now known that IscR is a global transcriptional regulator, controlling expression of approximately 40 genes[12]. Furthermore, this protein has the novel ability to recognize two different DNA motifs (type 1 and 2) based on cluster ligation[6,8,12]. Because Fe-S ligation is regulated *in vivo*[5,8], the Fe-S dependent changes in DNA binding specificity impart unexpected complexity to regulation of its target operons. The structure of *E. coli* IscR bound to one of its sites and analysis of IscR variants reported here revealed how a single DNA binding domain can make specific contacts with two distinct DNA binding motifs. Although the structure of the IscR-DNA complex exhibits some features expected of this class of wHTH proteins, unique features, such as the relocation of the specificity determinant Glu43, were identified, providing insight into how [2Fe-2S] cluster ligation can expand IscR target site selection.

Interactions of IscR with type 2 binding sites

The relatively small structural changes to both DNA and IscR protein that accompanied DNA binding suggest that apo-IscR is poised to bind the B-form DNA of the type 2 motif.

The interactions of Arg59 from the wing and Tyr41 from the recognition helix contributed substantial binding free energy, likely recognizing structural features of the *hya* DNA site. Base specificity was achieved by interactions between major groove cytosines (C_7C_8 and $C_{7'}C_{8'}$), purines (20 and 20') and thymines (19 and 19') with side chains from Glu43, Ser40 and Gln44, respectively, of the IscR DNA recognition helix (Fig. 6A). [2Fe-2S]-IscR showed similar sequence requirements for binding the type 2 site (data not shown) and likely binds in a similar conformation as apo-IscR (Fig. 6B).

While it is somewhat unusual to have an acidic residue, such as Glu43, featured at the center of a protein-DNA interface, this is not wholly unprecedented. Despite the prominent bidentate interaction that Glu43 formed with the C_7C_8 or $C_{7'}A_{8'}$ dinucleotide in each *hya* half site, this interaction contributed little to the binding free energy. This phenomenon is relatively well-appreciated; hydrogen bonds at protein-DNA interfaces often function to determine DNA binding specificity rather than mediate affinity[20,21,23]. Indeed, this appears to be the functional role of Glu43 in IscR.

[2Fe-2S] cluster ligation remodels the DNA binding domain

Although the Glu43 side chain played a key role in site-specific interactions of apo-IscR with the type 2 motif, it inhibited high affinity binding of the type 1 motif. We propose that an electrostatic clash between the carboxylate of Glu43 and the $T_{7'}T_{8'}$ dinucleotide, which is conserved in one half site of the type 1 motif, prevents close apposition of apo-IscR to the DNA, disrupting additional interactions between apo-IscR and the type 1 DNA. The resulting loss of free energy would prevent neutralization of the positive free energy contribution from desolvation of the glutamate residue (Fig. 6C). However, our finding that the E43A variant bypassed the requirement for Fe-S cluster ligation for high affinity binding to a type 1 site, suggests that at least part of the role of Fe-S cluster ligation is to remove the energetically unfavorable contribution of Glu43 to type 1 DNA binding. We propose that Fe-S cluster ligation induces a conformational change that repositions the specificity determinant Glu43 and allows additional specific and nonspecific contacts with the DNA that dictate binding affinity, thus broadening specificity. Cluster ligation likely reorients the negatively charged Glu43 away from the major groove to allow wild-type [2Fe-2S]-IscR binding with the type 1 site (Fig. 6D)

Although the structures studied here were of IscR lacking the cluster, the location of the cluster binding region provides a framework for considering the role of Fe-S cluster ligation in any conformational changes required for broadening DNA binding specificity. Electron density for the residues that encompass the cluster-binding region of IscR was either weak or missing in both the DNA and unbound IscR structures, indicating conformational flexibility of this region in the absence of the cluster. Therefore, stabilizing the region surrounding the cluster ligands (Cys92, Cys98, Cys104, and His107) upon Fe-S cluster ligation could result in movement of the dimerization helix to bring it nearer to the juxtaposed DNA binding domain of the opposing subunit. The resulting reorganization of the DNA binding domain in one subunit of [2Fe-2S]-IscR due to the impinging interactions from the dimerization helix of the other subunit could reorient the side chain of Glu43 for binding a type 1 site.

The structurally-similar [2Fe-2S] protein, SoxR, binds its target site as a dimer, although its mechanism of regulation differs from IscR. SoxR is only active as a transcriptional regulator in the oxidized $[2Fe\text{-}2S]^{2+}$ form[15], although both apo and $[2Fe\text{-}2S]^{+}$-SoxR are able to bind the same site with high affinity[24]. It has been proposed that oxidation of the cluster in one subunit of SoxR is able to transmit the signal to the DNA binding domain of the adjacent subunit, based on the interactions observed between the two domains in the structure of active SoxR bound to DNA [25]. In the case of SoxR, conformational changes upon oxidation of the [2Fe-2S] cluster of SoxR result in DNA bending for transcription activation[25].

In contrast, the oxidation state of the [2Fe-2S] cluster does not appear to play a role in the regulation of IscR activity[5]. Rather, changes in cluster occupancy, which are influenced by O_2 availability *in vivo*, lead to differential expression of IscR-dependent promoters based on the type of binding site[6,8]. Previous transcription profiling experiments carried out under aerobic and anaerobic conditions, which reflect the apo-IscR and [2Fe-2S] states of IscR, respectively, yielded very different IscR dependent responses and indicated a functional link to Fe-S homeostasis. For example, during anaerobic growth, when Fe-S clusters are stabilized, and demand for their synthesis is low, [2Fe-2S]-IscR binds type 1 sites to repress expression of the Fe-S biogenesis machinery[8,12]. Aerobically, Fe-S clusters are subject to higher turnover due to oxidative damage[26]. Therefore, apo-IscR predominates and binds type 2 sites to repress Fe-S cluster-containing anaerobic respiratory proteins and upregulates the alternative Suf pathway of Fe-S biogenesis [7,12,27]. Surprisingly, expression of most type 2 regulated promoters are additionally regulated under anaerobic conditions by other transcription factors, limiting the role of IscR to aerobic conditions. Thus overall, IscR-dependent regulation appears to exploit Fe-S cluster occupancy to differentially alter expression of genes under aerobic and anaerobic conditions through changes in DNA binding specificity.

In summary, IscR appears to represent a new paradigm for transcriptional regulation by Fe-S cluster-containing transcription factors. Although it is common for transcription factors to require a cofactor to regulate their activity, we are unaware of other transcription factors such as IscR that are active in both the apo and ligand-bound forms and use ligand binding to alter DNA binding specificity. Much of the current understanding of cofactor-containing transcription factors has been based on the analysis of only a subset of potential regulated promoters. As global studies of the binding and activity of transcription factors are pursued to identify genome wide targets, it is conceivable that a role for the apo-form of other transcription factors will be uncovered, as was the case for IscR[12]. Furthermore, metals may mediate other novel mechanisms of regulation. For example, in the case of the zinc regulator, Zur[28] from *Streptomyces coelicolor*, in addition to a structural zinc binding site, two zinc binding sites regulate DNA binding, with one site serving as an on/off switch for DNA binding and a second site that differentially tunes DNA affinity at target sites based on zinc binding if the “switch” site contains zinc. Thus, the study of metal binding transcription factors continues to provide a fascinating window into the role of metals in biology.

ONLINE METHODS

Strain construction

Plasmids expressing IscR variants were constructed by QuikChange site-directed mutagenesis (Agilent) of pPK6161 containing the gene for wild-type IscR under control of the T7 promoter[11]. The plasmids were subsequently transformed into PK7878 (BL21(DE3) Δ*himA*: :*tet* Δ*iscR*: :*kan*) for overexpression.

Protein Expression and Purification for Crystallography experiments

All constructs used in the crystallization trials were triple cysteine (C92/98/104A) variants. IscR-3CA constructs containing a C-terminal 6xHis tag were expressed and purified using similar protocols. Briefly, the pertinent IscR gene was transformed into BL21(DE3) cells and grown in LB media (or M9 minimal media, for selenomethionine incorporation) at 37°C. The cells were induced with 0.5 mM IPTG at an optical density of 0.5 at 600nm and harvested the next day by centrifugation. After lysing the cells with sonication, the protein was purified using GE Hiprep Ni^{+2} affinity column via the manufacturer's standard protocol. The fraction containing the pure protein was buffer exchanged into 25 mM Tris buffer at pH 7.5 containing 150 mM NaCl (or 500 mM NaCl in case of E43A mutant) using a GE HiPrep 26/10 desalting column. The protein was aliquoted, flash frozen and stored at −80°C if not used immediately.

Crystallization and data collection

Protein-DNA complexes were prepared by mixing purified IscR with *hya* DNA in a 1:1 molar ratio to a final concentration of 500 μM each. Multiple DNA oligodeoxynucleotides with different overhangs and lengths of DNA were tried in our crystallization screens with IscR-3CA, but good crystals (40×40×70μ) grew only from a 29bp DNA. Hence, this was also the DNA construct used for IscR-E43A-3CA mutant. DNA bound protein crystals were obtained using hanging drop vapor diffusion method by mixing the protein-DNA complex with an equal volume of solution containing 0.2 M ammonium sulfate (for IscR-3CA) or 0.2–0.3 M ammonium phosphate (for IscR-3CA, E43A), with 20% glycerol. IscR-3CA/*hya* complexes containing either 5'-iododeoxyuridine-labeled DNA or selenomethionine substituted apo-IscR were also crystallized under the same conditions as IscR-3CA/*hya* complex

Since IscR-3CA did not crystallize in the absence of *hya* DNA, the construct variant IscR-3CA(1-133) was generated by removing residues at the disordered C-terminus of IscR. Non-DNA-bound apo-IscR-3CA(1-133) crystals were obtained at room temperature using hanging drop vapor diffusion by mixing equal volumes of IscR-3CA(1-133) and a solution containing 2–2.2 M ammonium sulfate and 20% glycerol.

As all crystals grew in cryo-safe conditions, no external cryoprotectants were needed. Native and 5'-iododeoxyuridine labeled IscR-3CA/*hya* data sets were collected at the Advanced Light Source (ALS) beamlines 5.0.1 and 5.0.2, while A.L.S. beamline 8.2.2 was used to collect native datasets of the IscR-E43A-3CA/*hya* complex. IscR-3CA(1-133) native datasets were collected at ALS beamline 5.0.2. Se-Met data sets were collected at the

Advanced Photon Source (APS) NE-CAT beamlines 24-ID-C and 24-ID-E. Because the wild-type sequence lacked sufficient methionines to provide a strong anomalous signal for phase determination, additional methionines were introduced by substituting surface lysines at positions 51, 69, 103 and 159 with methionines[29,30]. Phase information was determined using Single-wavelength Anomalous Diffraction (SAD). The structure determined for Se-Met IscR-3CA/*hya* was used as a model to determine the structures of native IscR-3CA/*hya*, IscR-E43A/*hya* and IscR-3CA(1-133) using molecular replacement.

Structure determination and refinement

X-ray intensity data was processed either in iMOSFLM[31] and scaled using SCALA module in CCP4[32] or using HKL2000 and Scalepack[33]. The Solve[34] module in PHENIX[35] was used for heavy atom determination, and the Resolve[36] module was used for solvent flattening for the selenomethionine datasets. Autobuild module in PHENIX was used for initial model building with the rest of the model built manually using Coot[37]. A portion of the electron density map can be seen in Supplementary Fig. 5. For the IscR-E43A-3CA/*hya* complex and IscR-3CA(1-133), the PHASER[38] module in PHENIX was used for Molecular replacement to obtain phase information. TLS[39] refinement was used in the last round of refinement for all data sets. The structure coordinates and structure factors for IscR-3CA(1-133), IscR-3CA/*hya* and IscR-E43A-3CA/*hya* have been deposited at the RCSB with pdb accession code 4HF0, 4HF1 and 4HF2, respectively. Surface electrostatic potential was calculated by using PyMOL APBS (http://apbs.sourceforge.net) tools. All figures were prepared using Pymol software (The PyMOL Molecular Graphics System, Schrödinger, LLC) or CCP4MG[40]. For the structures of IscR/*hya*, IscR-E43A/*hya*, and IscR, 98.8, 96.5, and 99.1% of the bond angles fell within the allowed regions of the Ramachandran plot, respectively.

Purification of IscR for DNA binding experiments

Wild-type IscR and variants were anaerobically purified from PK8581 (wild-type), PK9034 (IscR-S40A), PK9036 (IscR-Y41A), PK9124 (IscR-E43A), PK9043 (IscR-Q44A), and PK9038 (IscR-R59A) as previously described for wild-type IscR[12]. As observed previously, anaerobically-isolated proteins were obtained as only partially occupied with [2Fe-2S] cluster (40–50% for wild-type IscR, 27–50% for mutants). Apo-IscR protein was generated by treatment of anaerobically-purified IscR with a 100-fold excess of EDTA under anaerobic conditions in the presence of a 10-fold excess of dithionite (DTH) at room temperature until there was no further decrease in absorbance at 420nm, corresponding to the complete loss of the [2Fe-2S] cluster. To concentrate IscR and remove residual EDTA, protein was bound to a gravity flow Biorex 70 column, washed with 10 mM HEPES (pH 7.4), 100 mM KCl, 10% glycerol, 1 mM dithiothreitol (DTT), and apo-IscR was eluted in 10 mM HEPES (pH 7.4), 1.0 M KCl, 10% glycerol, 1 mM DTT. Protein concentration was determined colorimetrically, as described previously[11]. To determine cluster occupancy, purified IscR was precipitated in an acidic solution, and the iron content of the cleared solution was determined colorimerically using the TPTZ method[41] and corrected for background Fe in the buffer. Assuming two moles of Fe bind per mole of IscR monomer containing a [2Fe-2S] cluster, a percentage of [2Fe-2S]-bound IscR was determined.

DNA-binding fluorescence polarization assays

DNA binding isotherms for binding of IscR variants to type 2 (*hya*) and type 1 (*iscRB*) binding sites were generated by measuring increases in fluorescence polarization upon binding of IscR to a 30 bp double-stranded DNA labeled on the 5' end of the top strand with the fluorophore, Texas Red (Integrated DNA Technologies). We then tested the binding of each variant protein to a 30 base pair DNA containing the same 29 base pair site that was crystallized with the apo-IscR mutant. The 30-mer double-stranded DNA contained either the 26-bp *hya* (5'-AT**AAATCCACACAGTTTGTATTGTTTTG**TG-3') or *iscRB* (5'-AA**ATAGTTGACCATTTTACTCGGGAATG**TC-3') binding site. Complementary strands of DNA were annealed as previously described[6].

To generate binding curves for IscR and its variants, increasing concentrations of either apo-IscR or anaerobically-isolated protein (containing 27–56% [2Fe-2S]-IscR) were incubated with 5nM labeled *hya* or *iscRB* DNA, as indicated. The protein was incubated with the labeled DNA in 40 mM Tris, pH 7.9, 150 mM KCl, 5% glycerol, 10 uM DTT for 12 minutes prior to measuring fluorescence polarization on a Beacon 2000 Fluorescence Polarization System (Invitrogen) using Texas Red filters (Andover Corporation). All manipulations were carried out under anaerobic conditions. To exclude ambient light, a 10 second delay prior to reading was used. When saturated binding to the labeled DNA was achieved, a four parameter Hill equation was used to fit the data (SigmaPlot version 12.0): $A = A_{free} + ((A_{bound} - A_{free})[IscR]^n)/(K_d^n + [IscR]^n)]$ in which A is the anisotropy, A_{free} is the anisotropy of unbound DNA, A_{bound} is the anisotropy under saturating binding conditions, $[IscR]$ is the concentration of IscR protein, and n is the Hill co-efficient. For a dimer-DNA binding model, the value of should be 1–2. The precise physical meaning of a value of n greater than 2 in this system is unknown. Nevertheless, the fitted value of n has no effect on the fitted value of K_d (supplementary fig. 7), which allowed us to make comparisons of K_d between variants, despite substantial differences in n. Although these substitutions appear far from the dimer interface, and wild-type IscR is a stable dimer by analytical ultracentrifugation at 12 and 49μM[6], an effect of the IscR monomer-dimer equilibrium on the K_d cannot be rigorously ruled out.

Equilibrium competition fluorescence assays were used to determine whether wild-type apo-IscR and apo-IscR-E43A discriminate at positions 7 and 8 of the *hya* site. In these assays, 8–1000 nM of competitor containing a single nucleotide mutation at position 7 or 8 was combined with 5 nM Texas Red labeled wild-type *hya* in 40 mM Tris-Cl (pH 7.9), 250 mM KCl, 5% glycerol, 10 uM DTT buffer under anaerobic conditions, 22 nM apo-IscR or 20 nM apo-IscR-E43A was added, then fluorescence was measured as described above. The fraction bound was determined using the equation $(A - A_{free})/(A_{bound} - A_{free})$, where A is the anisotropy of a sample, A_{free} is the anisotropy of the DNA in the absence of IscR, and A_{bound} is the anisotropy in the absence of competitor. The IC_{50} was determined by fitting a four parameter logistic curve to the data (SigmaPlot 12.0). All assays to generate binding isotherms and competition data were repeated on at least three independent occasions.

Supplementary Material

Refer to Web version on PubMed Central for supplementary material.

Acknowledgements

This work was funded by U.S. National Institutes of Health (NIH, GM045844) to P.J. Kiley and by The Methodist Hospital Research Institute to K.J. Phillips. The work was partly conducted at the Berkeley Center for Structural Biology (BCSB) beamlines at Advanced Light Source (ALS) and also at the Northeastern Collaborative Access Team (NECAT) beamlines at Advanced Photon Source (APS). BCSB is supported in part by the NIH, National Institute of General Medical Sciences, and the Howard Hughes Medical Institute. ALS is supported by the Director, Office of Science, and Office of Basic Energy Sciences, of the U.S. Department of Energy under Contract No. DE-AC02-05CH11231. This work is based upon research conducted at the APS on the NE-CAT beamlines, which are supported by grants from the National Center for Research Resources (5P41RR015301-10) and the National Institute of General Medical Sciences (8 P41 GM103403-10) from the NIH. Use of the APS, an Office of Science User Facility operated for the U.S. Department of Energy (DOE) Office of Science by Argonne National Laboratory, was supported by the U.S. DOE under Contract No. DE-AC02-06CH11357. We also thank the organizers and instructors of the 2012 CCP4 APS school attended by S. Rajagopalan for providing valuable insights in analyzing the data.

References

1. Johnson DC, Dean DR, Smith AD, Johnson MK. Structure, function, and formation of biological iron-sulfur clusters. Annu Rev Biochem. 2005; 74:247–81. [PubMed: 15952888]
2. Fleischhacker AS, Kiley PJ. Iron-containing transcription factors and their roles as sensors. Curr Opin Chem Biol. 2011; 15:335–41. [PubMed: 21292540]
3. Crack JC, Green J, Thomson AJ, Le Brun NE. Iron-sulfur cluster sensor-regulators. Curr Opin Chem Biol. 2012; 16:35–44. [PubMed: 22387135]
4. Guerra AJ, Giedroc DP. Metal site occupancy and allosteric switching in bacterial metal sensor proteins. Arch Biochem Biophys. 2012; 519:210–22. [PubMed: 22178748]
5. Fleischhacker AS, et al. Characterization of the [2Fe-2S] cluster of Escherichia coli transcription factor IscR. Biochemistry. 2012; 51:4453–62. [PubMed: 22583201]
6. Nesbit AD, Giel JL, Rose JC, Kiley PJ. Sequence-specific binding to a subset of IscR-regulated promoters does not require IscR Fe-S cluster ligation. J Mol Biol. 2009; 387:28–41. [PubMed: 19361432]
7. Yeo WS, Lee JH, Lee KC, Roe JH. IscR acts as an activator in response to oxidative stress for the suf operon encoding Fe-S assembly proteins. Mol Microbiol. 2006; 61:206–18. [PubMed: 16824106]
8. Giel JL, et al. Regulation of iron-sulphur cluster homeostasis through transcriptional control of the Isc pathway by [2Fe-2S]-IscR in Escherichia coli. Mol Microbiol. 2012
9. Rodionov DA, Gelfand MS, Todd JD, Curson AR, Johnston AW. Computational reconstruction of iron- and manganese-responsive transcriptional networks in alpha-proteobacteria. PLoS Comput Biol. 2006; 2:e163. [PubMed: 17173478]
10. Shepard W, et al. Insights into the Rrf2 repressor family--the structure of CymR, the global cysteine regulator of Bacillus subtilis. FEBS J. 2011; 278:2689–701. [PubMed: 21624051]
11. Schwartz CJ, et al. IscR, an Fe-S cluster-containing transcription factor, represses expression of Escherichia coli genes encoding Fe-S cluster assembly proteins. Proc Natl Acad Sci U S A. 2001; 98:14895–900. [PubMed: 11742080]
12. Giel JL, Rodionov D, Liu M, Blattner FR, Kiley PJ. IscR-dependent gene expression links iron-sulphur cluster assembly to the control of O2-regulated genes in Escherichia coli. Mol Microbiol. 2006; 60:1058–75. [PubMed: 16677314]
13. Lazazzera BA, Beinert H, Khoroshilova N, Kennedy MC, Kiley PJ. DNA binding and dimerization of the Fe-S-containing FNR protein from *Escherichia coli* are regulated by oxygen. J Biol Chem. 1996; 271:2762–8. [PubMed: 8576252]
14. Hidalgo E, Demple B. An iron-sulfur center essential for transcriptional activation by the redox-sensing SoxR protein. EMBO J. 1994; 13:138–46. [PubMed: 8306957]
15. Gaudu P, Weiss B. SoxR, a [2Fe-2S] transcription factor, is active only in its oxidized form. Proc Natl Acad Sci U S A. 1996; 93:10094–8. [PubMed: 8816757]

16. Ebright RH, et al. Role of glutamic acid-181 in DNA-sequence recognition by the catabolite gene activator protein (CAP) of Escherichia coli: altered DNA-sequence-recognition properties of [Val181]CAP and [Leu181]CAP. Proc Natl Acad Sci USA. 1987; 84:6083–7. [PubMed: 2888111]
17. Komori H, et al. Crystal structure of a prokaryotic replication initiator protein bound to DNA at 2.6 A resolution. EMBO J. 1999; 18:4597–607. [PubMed: 10469640]
18. MacPherson, S.; Larochelle, M.; Turcotte, B. Microbiol Mol Biol Rev. Vol. Vol. 70. United States: 2006. A fungal family of transcriptional regulators: the zinc cluster proteins; p. 583-604.
19. Reeves R, Nissen MS. The A.T-DNA-binding domain of mammalian high mobility group I chromosomal proteins. A novel peptide motif for recognizing DNA structure. J Biol Chem. 1990; 265:8573–82. [PubMed: 1692833]
20. Rohs R, et al. Origins of specificity in protein-DNA recognition. Annu Rev Biochem. 2010; 79:233–69. [PubMed: 20334529]
21. Rohs R, et al. The role of DNA shape in protein-DNA recognition. Nature. 2009; 461:1248–53. [PubMed: 19865164]
22. Haran TE, Mohanty U. The unique structure of A-tracts and intrinsic DNA bending. Q Rev Biophys. 2009; 42:41–81. [PubMed: 19508739]
23. Coulocheri SA, Pigis DG, Papavassiliou KA, Papavassiliou AG. Hydrogen bonds in protein-DNA complexes: where geometry meets plasticity. Biochimie. 2007; 89:1291–303. [PubMed: 17825469]
24. Ding H, Hidalgo E, Demple B. The redox state of the [2Fe-2S] clusters in SoxR protein regulates its activity as a transcription factor. J Biol Chem. 1996; 271:33173–5. [PubMed: 8969171]
25. Watanabe S, Kita A, Kobayashi K, Miki K. Crystal structure of the [2Fe-2S] oxidative-stress sensor SoxR bound to DNA. Proc Natl Acad Sci U S A. 2008; 105:4121–6. [PubMed: 18334645]
26. Imlay JA. Iron-sulphur clusters and the problem with oxygen. Mol Microbiol. 2006; 59:1073–82. [PubMed: 16430685]
27. Nesbit AD, Giel JL, Rose JC, Kiley PJ. Sequence-Specific Binding to a Subset of IscR-Regulated Promoters Does Not Require IscR Fe-S Cluster Ligation. Journal of Molecular Biology. 2009:28–41. [PubMed: 19361432]
28. Shin J, et al. Graded expression of zinc-responsive genes through two regulatory zinc-binding sites in Zur. PNAS. 2011; 108:5045–5050. [PubMed: 21383173]
29. Ohmura T, Ueda T, Hashimoto Y, Imoto T. Tolerance of point substitution of methionine for isoleucine in hen egg white lysozyme. Protein Eng. 2001; 14:421–425. [PubMed: 11477222]
30. Leahy DJ, Erickson HP, Aukhil I, Joshi P, Hendrickson WA. Crystallization of a fragment of human fibronectin: introduction of methionine by site-directed mutagenesis to allow phasing via selenomethionine. Proteins. 1994; 19:48–54. [PubMed: 8066086]
31. Battye TG, Kontogiannis L, Johnson O, Powell HR, Leslie AG. iMOSFLM: a new graphical interface for diffraction-image processing with MOSFLM. Acta Crystallogr D Biol Crystallogr. 2011; 67:271–81. [PubMed: 21460445]
32. The CCP4 suite: programs for protein crystallography. Acta Crystallogr D Biol Crystallogr. 1994; 50:760–3. [PubMed: 15299374]
33. Otwinowski Z, Minor W. Processing of X-ray diffraction data collected in oscillation mode. 1997; 276:307–326.
34. Terwilliger TC, Berendzen J. Automated MAD and MIR structure solution. Acta Crystallogr D Biol Crystallogr. 1999; 55:849–61. [PubMed: 10089316]
35. Adams PD, et al. PHENIX: a comprehensive Python-based system for macromolecular structure solution. Acta Crystallogr D Biol Crystallogr. 2010; 66:213–21. [PubMed: 20124702]
36. Terwilliger TC. Maximum-likelihood density modification. Acta Crystallogr D Biol Crystallogr. 2000; 56:965–72. [PubMed: 10944333]
37. Emsley P, Lohkamp B, Scott WG, Cowtan K. Features and development of Coot. Acta Crystallogr D Biol Crystallogr. 2010; 66:486–501. [PubMed: 20383002]
38. McCoy AJ, et al. Phaser crystallographic software. J Appl Crystallogr. 2007; 40:658–674. [PubMed: 19461840]

39. Painter J, Merritt EA. Optimal description of a protein structure in terms of multiple groups undergoing TLS motion. Acta Crystallogr D Biol Crystallogr. 2006; 62:439–50. [PubMed: 16552146]

40. McNicholas S, Potterton E, Wilson KS, Noble ME. Presenting your structures: the CCP4mg molecular-graphics software. Acta Crystallogr D Biol Crystallogr. 2011; 67:386–94. [PubMed: 21460457]

41. Fischer DS, Price DC. A simple serum iron method using the new sensitive chromogen tripyridyl-s-triazine. Clin Chem. 1964; 10:21–31. [PubMed: 14110802]

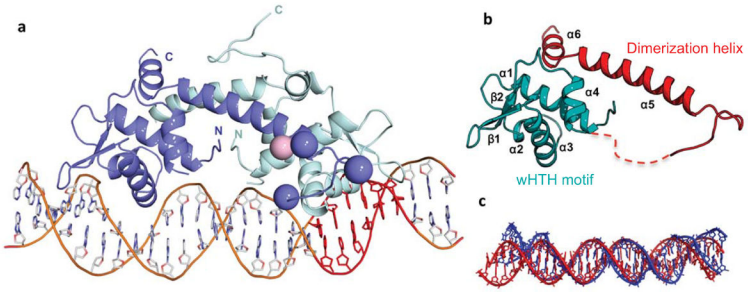

Figure 1.

Overall Structure of IscR bound to the *hya* promoter.

(a)The IscR dimer is shown as a ribbon representation, with the monomeric subunits colored purple and cyan and the DNA rendered as a stick model. The positions of the ligating residues in IscR are shown as large spheres with Ala92, Ala98, and Ala104 in purple and His107 in pink. This cluster binding region is in close proximity of to the wHTH DNA binding domain of the adjacent monomer. The −35 hexamer of the *hya* promoter is shown in red. Electron density is not apparent for residues beyond residue numbers 136 and 144 in the two IscR subunits for the subunits shown in purple and cyan, respectively.

(b) Cartoon representation of an IscR monomer. The dashed line indicates residues for which electron density was missing.

(c) Superposition of B-form DNA (red) and the IscR bound *hya* promoter (blue).

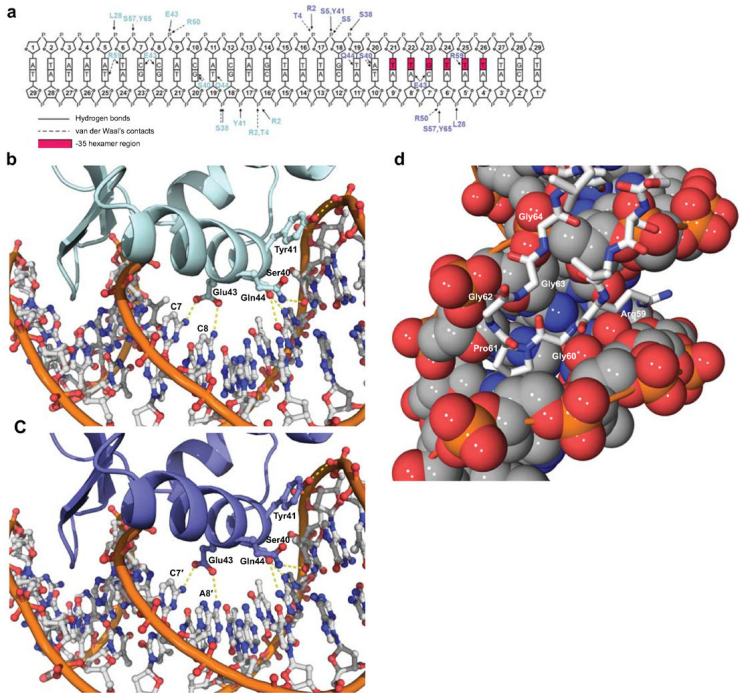

Figure 2.

IscR-*hya* DNA Interactions.

(a) Schematic representation of contacts between IscR and *hya* DNA. Contacts from each monomeric subunit of IscR are shown in cyan and purple, respectively.

(b, c) Residues involved in the interaction between the recognition helix of each monomer of IscR and the major groove of DNA. Yellow lines indicate hydrogen bonds.

(d) View of the interaction between the wing of IscR and the minor groove of DNA.

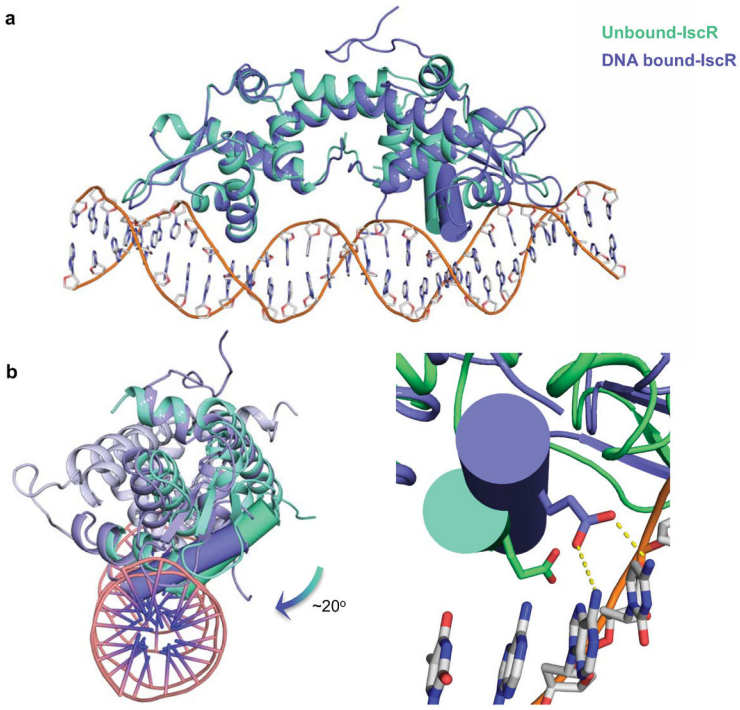

Figure 3.

IscR binding to the *hya* promoter involves only minor conformational changes.

(a, b) Superposition of the non-DNA bound IscR structure with that of IscR bound to the *hya* promoter. The recognition helix of one monomer from each structure is shown as cylinders.

(c) A close-up view showing the rotameric shift of the Glu43 side chain upon DNA binding.

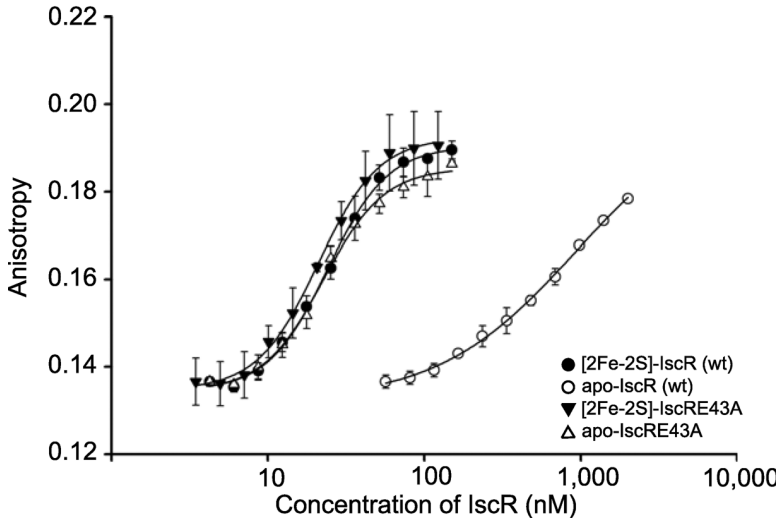

Figure 4.

Elimination of the Glu43 carboxyl group of apo-IscR broadens the DNA binding specificity to include type 1 sites.

Binding isotherms for wild-type [2Fe-2S]-IscR (filled circles), wild-type apo-IscR (open circles), [2Fe-2S]-IscR-E43A (filled triangles), or apo-IscR-E43A (open triangles) with a DNA containing the *iscRB* site. Error bars represent the standard deviation of at least three separate assays.

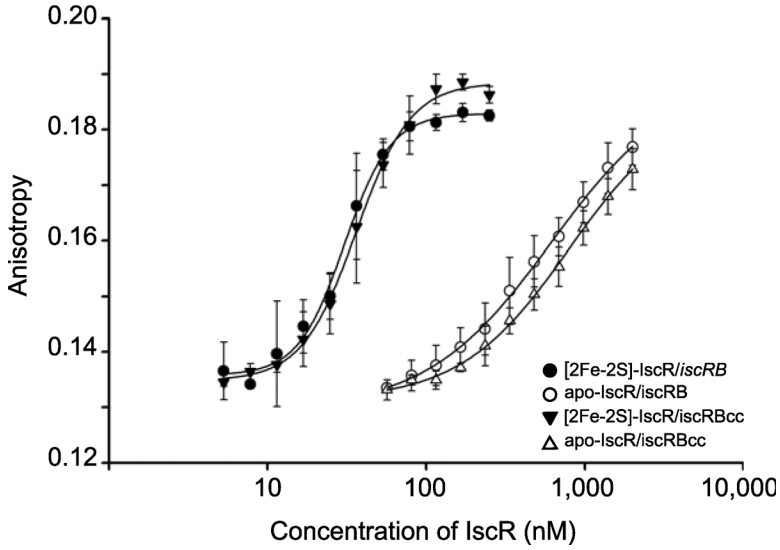

Figure 5.

Apo-IscR does not bind a type 1 site containing symmetrical cytosines at positions 7 and 8 of each half site.

Binding isotherms of [2Fe-2S]-IscR (filled circles) and apo-IscR (open circles) with the *iscRBcc* site (5'-AAATAG**CC**GACCATTTTACTCGGGAATGTC-3', mutated dinucleotide is bolded, symmetrical positions 7 and 8 are underlined). Error bars represent the standard deviation of at least three separate assays.

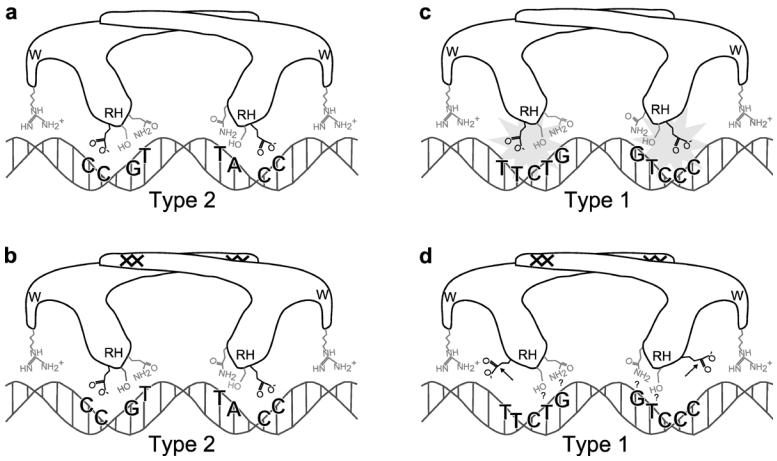

Figure 6.

Model for IscR discrimination between type 1 and type 2 motifs.

Interactions of apo and [2Fe-2S] IscR at type 1 and type 2 sites are shown. The side chains of Glu43 (black), Ser40 (gray), and Gln44 (gray) of the recognition helix (RH) make contacts to the DNA major groove and Arg59 (gray) of the wing (W) contacts the minor groove. A black diamond on IscR indicates the presence of a [2Fe-2S] cluster. The key nucleotides in the *hya* type 2 site or conserved positions in type 1 sites are represented in bold by A (adenine), T (thymine), C (cytosine), or G (guanine).

(a) The contacts between apo-IscR and the type 2 site. Glu43 of apo-IscR interacts with a C_7C_8 dinucleotide in one half site and $C_{7'}A_{8'}$ the other half site. Additional contacts are made by Arg59 with the minor groove, Ser40 with an A or G, and Gln44 with T.

(b) The contacts between [2Fe-2S]-IscR and the type 2 site are the same for apo-IscR, described in panel a.

(c) The lack of interaction of apo-IscR with the type 1 site is indicated by the starburst.

(d) The contacts between [2Fe-2S]-IscR and the type 1 site. Displacement of the Glu43 (black) side chain from the major groove is indicated by the outward-pointing arrows. The interaction of Arg59 with the minor groove is the same as in panels a and b. Question marks represent uncertainty about the site of the interaction of Ser40 and Gln44 with conserved nucleotides in the type 1 site.

Table 1

Data collection and refinement statistics

	IscR-DNA (Se-Met SAD)[a]	IscR-DNA	IscR^{E43A}-DNA	IscR
Data collection				
Space group	$P2_12_12_1$	$P2_12_12_1$	$P2_12_12_1$	$P3_121$
Cell dimensions				
a, *b*, *c* (Å)	49.12, 74.92, 187.14	49.12, 75.32, 187.39	48.62, 75.18, 186.45	88.85, 88.85, 62.73
α, β, γ (°)	90, 90, 90	90, 90, 90	90, 90, 90	90, 90, 120
Resolution (Å)	26.96–2.90 (3.00–2.90)[b]	48.08–2.22 (2.30–2.22)	43.11–2.99 (3.10–2.99)	48.62–1.90 (1.97–1.90)
R_{sym} (%)	7.7 (44.8)	7.1 (59.6)	9.5 (56.0)	5.7(61.2)
I / σI	34.72 (10.68)	17.57 (5.04)	15.36 (5.15)	16.89 (2.78)
Completeness (%)	99.6 (98.3)	94.0 (72.1)	98.8 (95.0)	99.98 (100.00)
Redundancy	10 (9.5)	7.0 (5.4)	6.7 (5.3)	8.7 (8.7)
Refinement				
Resolution (Å)		2.22	2.99	1.90
No. reflections		27065 (1114)	12074 (612)	22775 (2244)
R_{work} / R_{free}		20.28/22.79	22.94/26.11	19.33/22.05
No. atoms				
Protein		1913	1744	1743
DNA		1183	1183	0
Ligand/ion		0	0	5
Water		0	0	37
B-factors				
Protein		57.90	89.27	30.90
DNA		87.50	122.48	0
Ligand/ion		0	0	58.986
Water		0	0	35.10
r.m.s. deviations				
Bond lengths (Å)		0.004	0.004	0.008
Bond angles (°)		1.01	1.02	0.98

[a] One crystal was used per data set.

[b] Values in parentheses are for highest-resolution shell.

Table 2

Alanine substitutions in the DNA recognition helix of IscR decrease binding affinity for *hya*

IscR variant	Binding affinity (K_d)[a] nM	Hill slope (n)[b]	Maximum anisotropy (A_{max})[c]	% wild-type binding activity
wild-type	17 ± 1[d]	3.7 ± 0.2	0.19 ± 0.01	100
S40A	170 ± 5	2.5 ± 0.2	0.18 ± 0.01	10
Y41A	>300	2.3 ± 0.2	0.18 ± 0.01	<6
E43A	22 ± 1	4.0 ± 0.5	0.19 ± 0.01	80
Q44A	57 ± 2	2.5 ± 0.2	0.19 ± 0.01	30
R59A	>500	1.8 ± 0.1	0.19 ± 0.01	<4

*a, b, c*The Binding affinity (K_d), Hill slope (n), and maximum anisotropy (A_{max}) for each variant protein with the *hya* site was determined from DNA binding isotherms shown in Supplementary Fig. 2.

*d*The standard deviation is derived from fitting a four parameter Hill equation to the average of at least three independent binding experiments for each variant.

Table 3

IscR-E43A does not discriminate for a cytosine dinucleotide at positions 7 and 8 in mutant *hya* sites

Competitor	Sequence	IC_{50}[a] with IscR/*hya*	IC_{50} with IscR-E43A/*hya*
hya	ATAAATCCACACAGTTTGTATTGTTTTGTG[b]	32 ± 2[c]	11 ± 1
shuffled	AT**CATCCGTCTTATGTTAATTATAATGG**TG[d]	>1000	>1000
hya (7C to G)	ATAAATGCACACAGTTTGTATTGTTTTGTG	>510	17 ± 3
hya (8C to G)	ATAAATCGACACAGTTTGTATTGTTTTGTG	>740	7 ± 3
hya (8C to A)	ATAAATCAACACAGTTTGTATTGTTTTGTG	>1000	6 ± 1
hya (8C to T)	ATAAATCTACACAGTTTGTATTGTTTTGTG	>1000	8 ± 1

[a] The concentration of unlabeled mutant competitor required to decrease maximum binding (A_{max}) to labeled *hya* DNA by a factor of 0.5 (IC_{50}).

[b] Positions 7 and 8 are underlined.

[c] The standard deviation is derived from fitting a four-parameter logistic curve to the average of at least three independent titration experiments.

[d] Mutations in each competitor sequence are bolded.

Table 4

Alanine substitutions in the DNA recognition helix of IscR decrease binding affinity for *iscRB*

IscR variant	Binding affinity (K_d)[a] nM	Hill slope (n)[b]	Maximum anisotropy (A_{max})[c]	% wild-type binding activity
wild-type	24 ± 1[d]	2.3 ± 0.8	0.19 ± 0.01	100
S40A	94 ± 3	1.5 ± 0.1	0.18 ± 0.01	26
Y41A	>2000	1.3 ± 0.3	0.18 ± 0.01	<1
E43A	21 ± 1	2.3 ± 0.2	0.19 ± 0.01	115
Q44A	>600	1.3 ± 0.1	0.21 ± 0.01	<4
R59A	n.d.[e]	n.d.	n.d.	<1

*a, b, c*The Binding affinity (K_d), Hill slope (n), and maximum anisotropy (A_{max}) for each variant protein with the *iscRB* site was determined from DNA binding isotherms (shown in Supplementary Fig. 2). Purified variant IscR proteins were incubated anaerobically with a DNA containing the *iscRB* site.

*d*The given standard deviation is derived from fitting a four parameter Hill equation to the average of at least three independent binding experiments for each variant.

*e*No observable binding at the IscR protein concentrations tested.